2021

Characterization of a Label-free Fluorescent Assay for Point Mutation Discrimination Based on Split Aptamer Probes

Shannon A. Beaton
University of Central Florida

CHARACTERIZATION OF A LABEL-FREE FLUORESCENT ASSAY FOR POINT MUTATION DISCRIMINATION BASED ON SPLIT APTAMERS

by

SHANNON A. BEATON
B.S. University of Central Florida, 2021

A thesis submitted in partial fulfillment of the requirements
for the Honors in the Major program in Biochemistry
in the Department of Chemistry
in the College of Sciences
and in the Burnett Honors College
at the University of Central Florida
Orlando, Florida

Spring Term, 2021

Thesis Chair: Dr. Yulia Gerasimova, Ph.D

ABSTRACT

Due to the misuse of antibiotics, multi-drug resistant (MDR) bacteria have become more rampant in our society; these MDR have given rise to diseases that are not readily curable. One such agent is the *Mycobacterium tuberculosis* complex, which is a causative agent of tuberculosis (TB). Timely diagnostics of the bacterial infection and detection of bacterial drug-susceptibility profiles helps to initiate the necessary treatment in a timely fashion and to limit transmission of the disease. For more affordable detection of bacterial diseases, tag-free split aptamer probes are promising. This research aims at characterizing split aptamer probes for detection of point mutations in the rpoB and katG genes of *M. tuberculosis* that are associated with resistance to two front-line antibiotics – rifampin and isoniazid, respectively, which causes MDR-TB. The probes have been designed and tested with synthetic oligonucleotide mimics of the bacterial genes in terms of their limit of detection and selectivity in discriminating the targets with single-nucleotide substitutions.

ACKNOWLEDGEMENTS

First and most importantly, I would like to thank my thesis chair, Dr. Yulia Gerasimova for accepting me into her research team and allowing me to do this research. Without her aid and support of me as a young researcher I would not have been able to complete my thesis. Dr. Gerasimova worked closely with me correcting and explaining concepts to help me produce this work as well as aiding in helping me to become a better scientist. I want to let my deepest appreciation be known for all your work and inspiration.

Additionally, I would like to thank Ryan Connelly, for supervising and training me in the lab. Mr. Connelly was always available to explain my data at critical moments during my research, as well as providing me with the images I needed. He is currently a graduate student who has, without a doubt be instrumental in helping me feel less of an imposter in my journey to becoming a researcher.

Finally, I would like to thank God, my family, and friends, for supporting me as I kept striving to complete not only my thesis but my degree. Without their words of wisdom, I would not be as far as I am today. Thank you!

TABLE OF CONTENTS

CHAPTER 1: INTRODUCTION

Differentiation of highly homologous nucleic acid targets is important in disease diagnostics and analysis of factors determining people's predispositions to diseases (Wang et al. 1998), genotyping of infectious agents (Versalovic and Lupski 2002), identity testing, among others. In some applications, as little difference in nucleic acid sequences as single-nucleotide substitutions needs to be reliably analyzed. For example, one of the mechanisms of bacterial resistance to antibiotics is by acquiring point mutations in bacterial genes encoding drug targets or enzymes responsible for pro-drug activation (Davies 2007). In some cases, mutations occur in several genes resulting in bacterial isolates exhibiting resistance to several antibacterial drugs simultaneously. Such cases are examples of multi-drug resistance (MDR) (Nikaido, 2009), which has become one of the greatest medical threat of mankind. For example, multi-drug-resistant tuberculosis (MDR-TB) has been assessed by the World Health Organization (WHO) as recently as 2019 as still being one of the top 10 causes of death worldwide. Despite improvements of the detection percentage from 48% in 2017 to 51% in 2018, only one in three of this 51% could be enrolled for treatment of MDR-TB (WHO, 2019) as a result of slow detection responses worldwide. This is due to the lack of affordable and yet fast and reliable tools for bacterial drug-susceptibility testing (DST). Prompt detection of MDR-TB cases allows medical providers to make informed decisions regarding appropriate anti-TB treatment in a timely fashion.

Currently, a WHO-supported solution for fast identification of *Mycobacterium tuberculosis*, a causative agent of TB, and analysis of its resistance to one of the first line antituberculosis drugs – rifampin - is the Cepheid Xpert MTB/RIF Ultra assay (Chakravorty et al. 2017). It uses real-

time PCR for amplification of a rpoB gene fragment from *M. tuberculosis* complex serving as a "hot spot" for point mutations causing rifampin resistance, and five molecular beacon (MB) probes to interrogate the amplified fragment in a multiplex fashion (Helb et al. 2010). MB probes are stem-loop folded oligonucleotides conjugated with a fluorophore and a quencher dye at the opposite terminal (Tyagi and Kramer, 1996). In the absence of a target complementary to the loop portion of the probe, the MB probe is in the closed folded conformation, in which the fluorophore is adjacent to the quencher, and the fluorescent signal is low. Hybridization of the probe with the specific nucleic acid target results in the opening of the stem-loop and formation of the probe-target hybrid, in which the fluorophore is away from the quencher, and fluorescence is increased. It was demonstrated that the MB probe is superior in terms of specificity of target recognition as compared with monolith unstructured hybridization probes (Bonnet et al. 1999).

Despite the success of MB probes in molecular diagnostics, they suffer from some limitations. For example, the probes require covalent attachment of two dyes to the opposite ends of the oligonucleotide probe sequences. This increases the cost of the probe, both at the assay optimization stage and of the final product. Label-free nucleic acid detection is advantageous in this respect. It can be realized with the help of fluorescent light-up aptamers (FLAPs) (Neubacher et al, 2019). Aptamers are nucleic acids sequences that fold into a tertiary structure to allow for the formation of a specific binding pocket for their cognate ligands (Navani and Li, 2006). The ligand for FLAPs is a fluorogenic dye with inherently low fluorescence, which exhibits enhanced fluorescence upon binding to the aptamer (Rossetti, 2019).

To combine the advantage of label-free fluorescence detection that FLAPs offer with high selectivity required for point-mutation differentiation, we proposed to use a split approach for the

design of FLAP-based hybridization probes. Split probes consist of at least two components interrogating a nucleic acid target simultaneously. High signal can be achieved only when both components are fully complementary to the analyzed target (Kolpashchikov 2010). This requirement allows for a design of a probe that can simultaneously tightly bind the target and be selective to small differences in the target's sequence, thereby overcoming a notorious affinity-specificity dilemma (Demidov and Frank-Kamenetskii, 2004). Indeed, MB-based split probes were shown to exhibit selectivity under broader conditions than the MB probes themselves (Stancescu et al. 2016).

Objective

The goal of this study is to characterize two split aptamer probes for the detection of the katG and rpoB gene fragments from *M. tuberculosis* and discrimination of the nucleic acid target sequences corresponding to drug-susceptible from drug-resistant bacterial phenotypes. We hypothesized that the probes can selectively detect their cognate targets both when used separately and in a multiplex format.

CHAPTER 2: METHODOLOGY

2.1. Materials and instruments

All oligonucleotides were acquired from Integrated DNA Technologies (Coralville, IA, USA). Tris base was purchased from Sigma-Aldrich (St. Louis, MO). The dye Auramine-O (AO) and N-methylmesoporphyrin (NMM) purchased from ThermoFisher Scientific (Waltham, MA). Hydrochloric acid (HCl) and nuclease-free water were purchased from Fisher Scientific (Waltham, MA).

To prepare a buffer used in fluorescent assays, a solution of Tris base (1 M) was prepared in water, and its pH was adjusted to 7.4 by titrating it with concentrated HCl.

Oligonucleotides were dissolved in water. Concentrations of oligonucleotide stock solutions were calculated based on their absorption at 260 nm using a NanoDrop OneC Microvolume UV-Vis Spectrophotometer (ThermoFisher Scientific, Waltham, MA).

The fluorescence emission spectra of the samples in a quartz cuvette with a 3 mm path length were recorded in 420-640 nm range upon excitation at 399 nm and/or 475 nm (excitation/emission slits 10/20 nm) using the Cary Eclipse fluorescence spectrophotometer (Agilent, Santa Clara, CA). The signal at 540 nm for AO and 608 nm for NMM was used for the data analysis.

2.2. Fluorescence assay based on the katG-specific split dapoxyl aptamer (SDA) probe

Eleven samples of 60 µL were prepared, containing 3 µL of 10 µM each of SDA_U strand and SDA_S strand, 1 µL of 120 µM Auramine-O in ethanol, 30 µL of the assay buffer×2 (40 mM Tris-HCl, pH 7.4, 40 mM KCl, 50 mM $MgCl_2$ and 2% DMSO) and nuclease-free water up to 50 µL.

To nine of the samples, 10 µL of 0.048 µM, 0.096 µM, 0.192 µM, 0.384 µM, 0.768 µM, 1.536 µM, 3.072 µM, 4.608 µM or 6.144 µM katG_WT was added. One sample contained 10 µL of 6.144 µM katG_315C, and a final blank sample was prepared with 10 µL nuclease-free water. The samples were incubated at 25°C temperature for 20 mins before being measured in the spectrofluorometer.

2.3. Fluorescent assay based on the rpoB-specific split G-quadruplex (SGQ) probe

Twelve samples of 60 µL were prepared, containing 6 µL at 10 µM each of SGQ_U strand and SGQ_S strand, 1 µL of 120 µM NMM in ethanol, 30 µL of the assay buffer×2 (40 mM Tris-HCl, pH 7.4, 40 mM KCl, 50 mM $MgCl_2$ and 2% DMSO) and nuclease-free water up to 50 µL. To nine of the samples, 10 µL of 0.048 µM, 0.096 µM, 0.192 µM, 0.384 µM, 0.768 µM, 1.536 µM, 3.072 µM, 4.608 µM or 6.144 µM rpoB_WT was added. One sample contained 10 µL of 6.144 µM rpoB_C>G_526, one contained 10 µL of 6.144 µM rpoB_C>T_526 and a final blank sample was prepared with 10 µL Nuclease-free water. The samples were incubated at 25°C temperature for 20 mins before being measured in the spectrofluorometer.

2.4. Multiplex fluorescent assay

Samples (60 µL) were prepared by mixing1 µL of 120 µM Auramine-O in ethanol, 1 µL of 120 µM NMM in ethanol, 30 µL of the assay buffer×2 (40 mM Tris-HCl, pH 7.4, 40 mM KCl, 50 mM $MgCl_2$ and 2% DMSO), indicated combinations of the SDA and/or SQG probes (at 0.5 µM or 1 µM final concentration, respectively) and nuclease-free water up to 50 µL. To the samples, 10 µL of 6.144 µM katG_315_WT; 10 µL of 6.144 µM rpoB_WT, 10 µL of 6.144 µM katG_315_WT/ rpoB_WT mixture or 10 µL of nuclease-free water was added. The samples were incubated at

25°C temperature for 20 mins before being measured in the spectrofluorometer. Fluorescence spectra of each sample were recorded twice – upon excitation at 399 nm and at 475 nm.

2.5. Oligonucleotide Sequences

Table 1: Oligonucleotides used in this study

Name	**Sequence**[a]
SDA_U	TGTTCGTCCATACGACCTCGATGTTCTACGGGGGAGGGTGTGTGGTTTTGGTCAT
SDA_S	ATGACCTTGGTTCGTAGTTCCGCTGCTG
katG_WT	AACCGGTAAGGACGCGATCACCAGCGGCATCGAGGTCGTATGGACGAACACCCCGACGAAATGGGACAACAGTTTCCTCG
katG_315C	AACCGGTAAGGACGCGATCACCACCGGCATCGAGGTCGTATGGACGAACACCCCGACGAAATGGGACAACAGTTTCCTCG
SGQ_U	GGGTTGGG/iSp9/AACCCCAACAGCGGGTTGT
SGQ_S	CCCTATTGTGGGTC/iSp9/GGGTAGGG
rpoB_WT	GGACCAGAACAACCCGCTGTCGGGGTTGACCCACAAGCGCCG
rpoB_C>T	GGACCAGAACAACCCGCTGTCGGGGTTGACCTACAAGCGCCG
rpoB_C>G	GGACCAGAACAACCCGCTGTCGGGGTTGACCGACAAGCGCCG
DAP-10-42	CAATTACGGGGGAGGGTGTGTGGTCTTGCTTGGTTCTTCGTATTG

[a]/iSp9/ is triethylene glycol linker; nucleotides of the target-binding fragments of strands U and their complementary target fragments are in orange; nucleotides of the target-binding fragments of strands S and their complementary target fragments are in green; point-mutation sites are in bold; intra- and intermolecular self-complementary fragments of SGQ_S, SDA_U and SDA_S strands are underlined.

CHAPTER 3: RESULTS

3.1 Design of Split Aptamer Probes

To design aptamer probes, two DNA aptamers were used as a scaffold – the dapoxyl binding aptamer (DA) (Kato et al. 2016) and a G-quadruplex (GQ) forming sequence that binds *N*-methyl mesoporphyrin IX (NMM) (Scheme 1A) (Yett et al. 2019). For the DA-based probe, we used auramine O (AO) dye (Scheme 1B) as a fluorogen. The dye-binding fragments of DA and GQ were split in two parts and elongated with target-binding fragments to form split aptamer probes SDA and SGQ, respectively. Specifically, DA was split between nucleotide (nts) 28 and 29 of the parent aptamer sequence (Scheme 2), which was previously shown to allow for the re-forming of the dye-binding pocket of the aptamer in the presence of a cognate nucleic acid target (Kikuchi et al. 2019). The GQ forming sequence was split so that each strand of the probe contained two G-triplets (Table 1). The G-rich fragments of the SGQ probe strands were connected to the target-binding fragments via triethylene glycol linkers to ensure formation of the GQ motif next to the double-stranded domain of the probe-target complex. In addition, SGQ_S strand contained a 5'-terminal fragment complementary to its GQ-forming fragment to improve selectivity of rpoB-WT recognition. The SGQ probe was previously used for colorimetric detection of *Mycobacterium tuberculosis* when the peroxidase-like catalytic activity of parallel GQ sequences was explored (Connelly et al., 2018; Connelly et al. 2019). The SDA probe was tailored to recognize the wild-type sequence of the katG gene fragment bearing a point mutation site in the codon 315 associated with isoniazid resistance. The SGQ probe was designed for interrogation of the wild-type sequence of a "hot-spot" fragment of the rpoB gene with a point mutation site in the codon 526. Substitution of C at this position of the rpoB gene to either G or T was shown to be one of the predominant causes of bacterial resistance to rifampin.

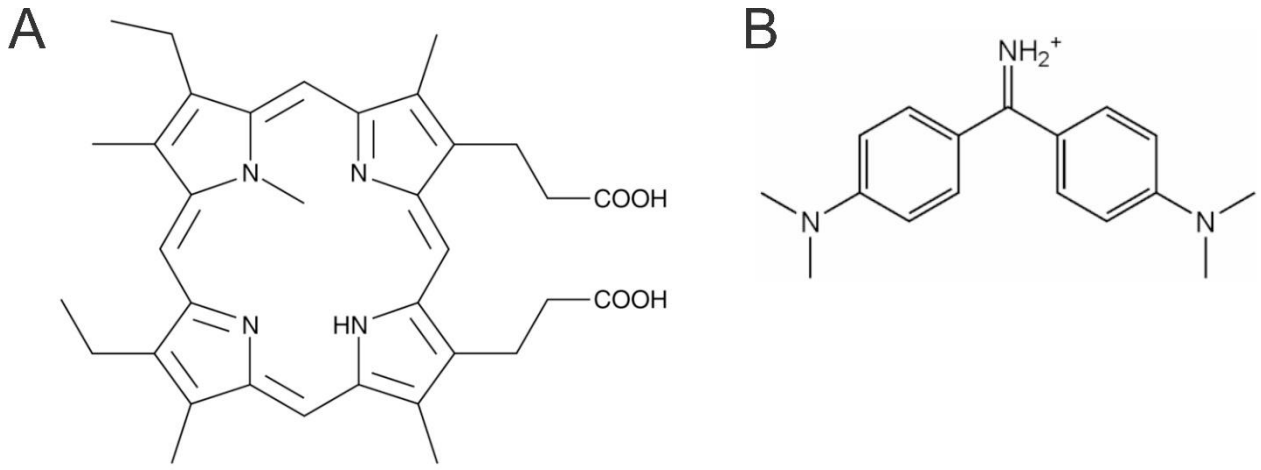

Scheme 1. Chemical structures of NMM (A) and AO (B) – fluorogenic dyes used in conjunctions with the aptamer probes in this study.

Each split probe consisted of strand U and strand S with their target-binding fragments complementary to the adjacent positions of the respectful genes (Scheme 3, Table 1). The target-binding fragment of strand S was complementary the fragment with the correspondent point-mutation site. To ensure formation of the dye-binding site only in the presence of the fully complementary but not the single-base mismatched nucleic acid target, the target-binding fragment of strand S of the probes was shortened to 9 nts to ensure T_m of the hybrid formed between strand S and the mismatched target to be below the assay temperature (25^{o}C). The probe design was assisted by the analysis of the stability of the target-probe complexes *in silico* using NUPACK software (Zadeh et al. 2011). The sequences of the probe strands allowing for the assembly of the target-probe complex only in the presence of the fully complementary wild-type target sequence were chosen for experiments.

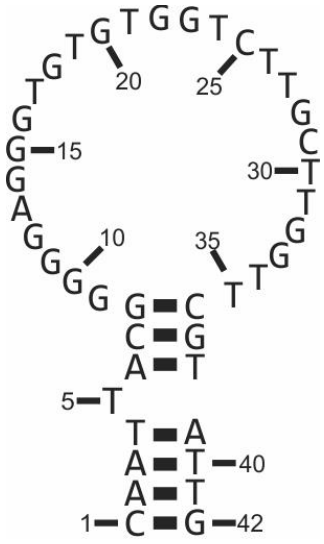

Scheme 2. Minimal energy secondary structure of the dapoxyl binding aptamer DAP-10-42 predicted by NUPACK software (Zadeh et al. 2011).

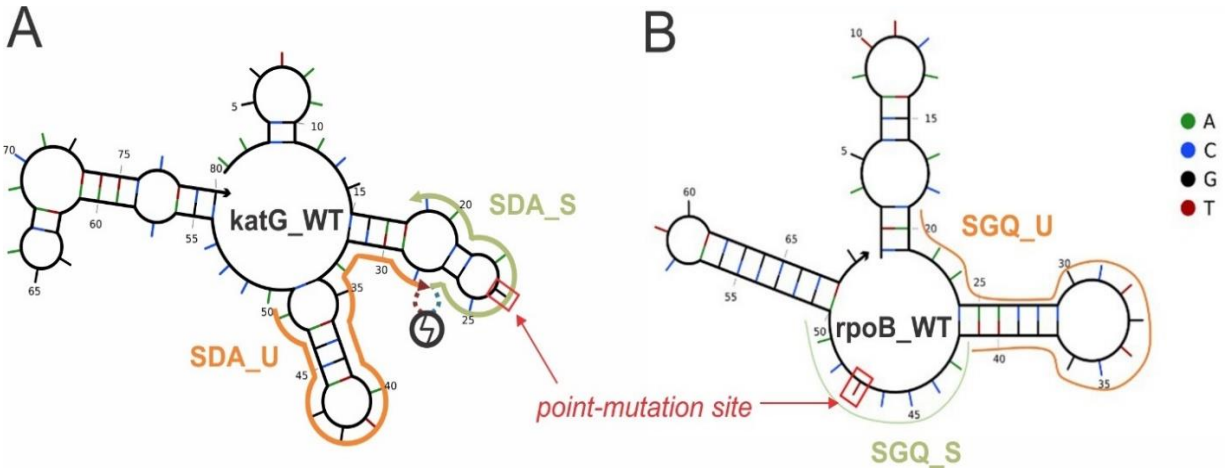

Scheme 3. Minimal energy secondary structures for katG-WT (A) and rpoB_WT (B) targets. The point-mutation sites are indicated by a red box. The fragments of the targets complementary to strands U and S of their cognate probes are shown by orange and green curves, respectively.

3.2 Performance of the SDA probe

The designed SDA probe was tested using increased concentrations of a synthetic mimic of the katG gene – katG-WT (Table 1). The fluorescent signal at 540 nm upon excitation at 475 nm was measured in the presence of the increased katG-WT concentration (Figure 1). It can be seen that the signal intensity increases with the target concentration in the range of 0-512 nM and then drops when the target's concentration exceeds the concentration of the SDA strands. The drop can be explained by binding of the excess of the target to each of the two strands of the probe independently rather that binding to both under this stoichiometry. As a result, the amount of the tripartite complex target-U-S, which is responsible for high signal, decreases (Scheme 3A).

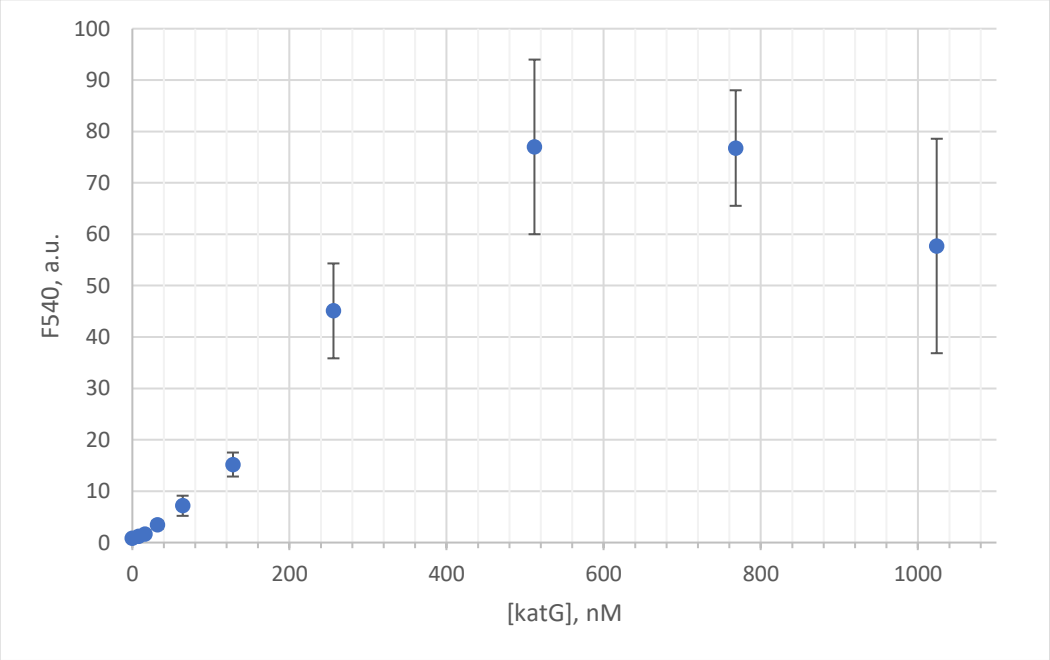

Figure 1. Fluorescence of AO in the presence of the katG-specific SDA probe as a function of katG_WT concentration (0-1024 nM). The data is averaged from at least three independent experiments, and error bars are provided as standard deviations from the average.

Linear dynamic range for the katG_WT detection with the cognate SDA is 1-512 nM. The limit of detection (LOD) and limit of quantification (LOQ) was determined from the data in the presence of 0-64 nM katG_WT (Figure 2) using the 3σ/S and 10σ/S rule, respectively (Dolatto, 2012), where σ is the standard deviation from the blank (the sample with no target added), and S is the slope of the linear trendline. For the SDA probe, the LOD of 2.6±0.6 nM and the LOQ of 9±2 nM was calculated.

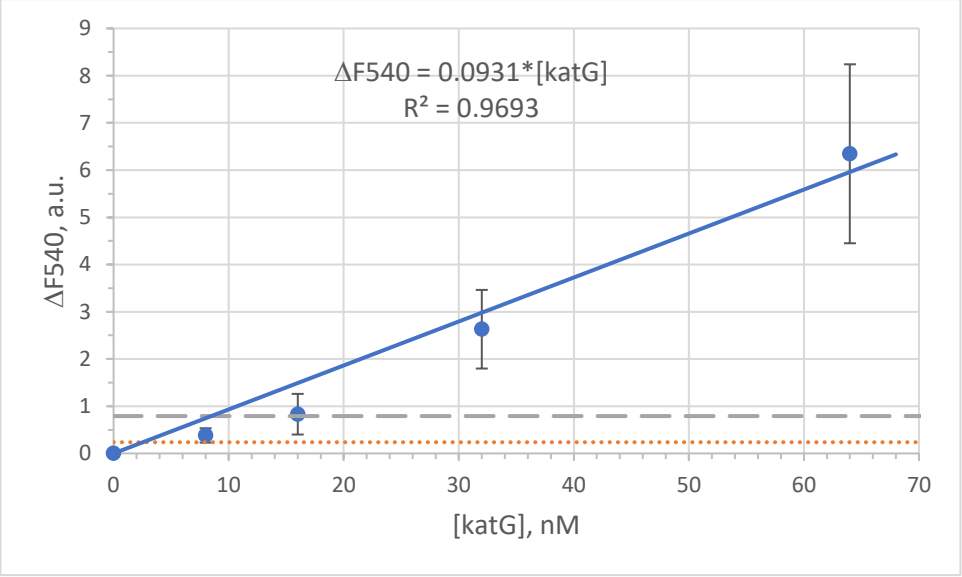

Figure 2. Linear dynamic range for the katG-specific SDA probe. The fluorescence thresholds corresponding to LOD and LOQ are shown with orange dotted and grey dashed lines, respectively. The data of four independent experiments is averaged. The error bars are given as standard deviations from the average. The signal is expressed in DF=F-F_{Blank}, where F_{Blank} is the signal in the absence of the target.

The SDA probe with the AO dye exhibits low fluorescence in the absence of its cognate target and a bright target-triggered signal. The signal can be even observed by the unaided eye when visualized using a hand-held UV lamp (excitation at 365 nm) (Figure 3). It can be seen that the signal triggered by 128 nM target or higher can be reliably distinguished from the blank even without the use of the fluorometer for the signal monitoring.

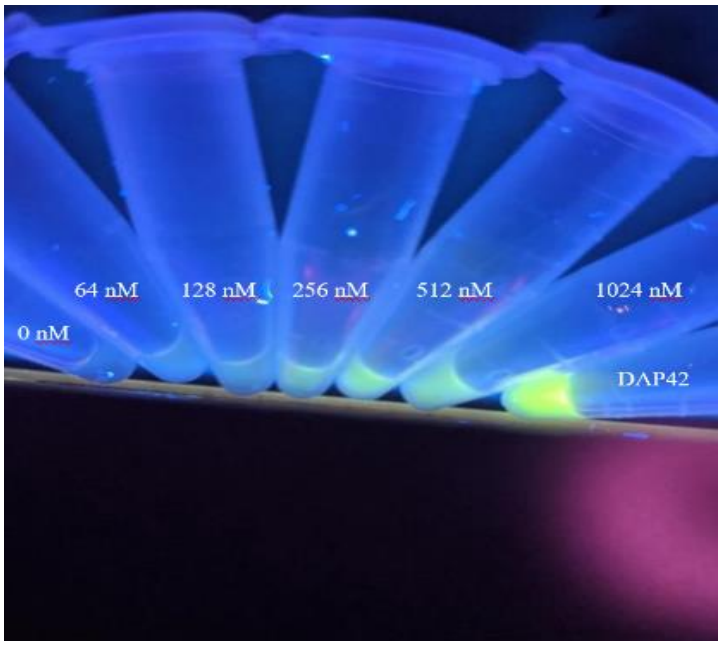

Figure 3. Images of the tubes of the SDA samples containing 1 µM strands, 20 µM AO in a buffer containing 20 mM Tris HCl- 7.4 pH, 20 mM KCl, 25 mM $MgCl_2$ and 1% DMSO at different katG_WT concentrations (0, 64, 128, 256, 512 or 1024 nM) were taken using a smartphone camera upon excitation with a hand-held UV-lamp of 365 nm. The rightmost tube contains 1µM DAP42 (monolith aptamer) in the presence of 20 µM AO in the same buffer.

Next, we tested the selectivity of the katG-specific SDA probe. Figure 4 shows the signal triggered by a mismatched target katG-315-G>C as compared with the signal triggered by the cognate katG_WT target (Table 1). As expected, the mismatched target failed to increase the fluorescence of the SDA/AO probe above the background level (Figure 4, compare bars for "Blank" and "katG-315-G>C). At the same time, the signal in the presence of katG_WT (1 µM) was ~60-fold higher than the blank.

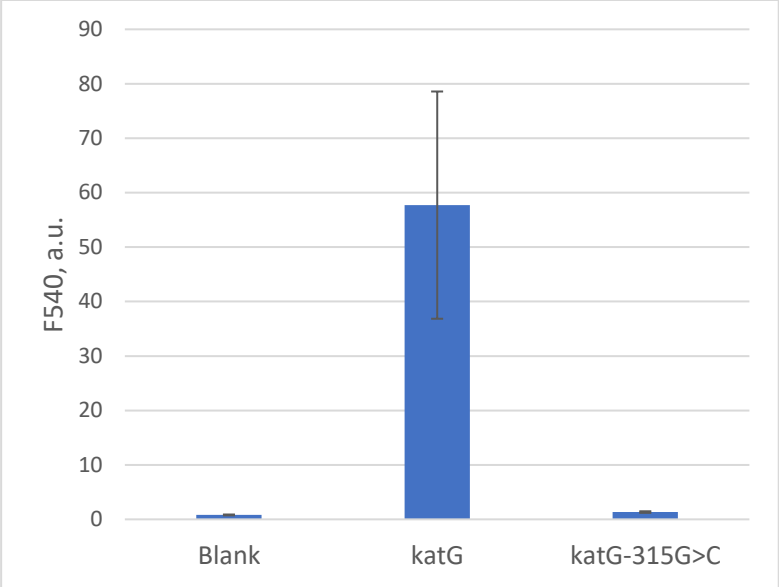

Figure 4. Selectivity of the katG-specific SDA probe using AO as a signal indicator. The targets (either specific katG_WT or single-nucleotide substituted katG-315-G>C) were at 1 μM. Blank represents the sample of the probe in the absence of the targets. The data of at least three independent experiments was averaged, and the standard deviations were shown as error bars.

3.3: Performance of the SGQ Probe

The designed rpoB-specific SGQ probe was tested using rpoB_WT – a synthetic mimic of the correspondent fragment of the rpoB gene from *M. tuberculosis*. The fluorescent signal at 608 nm upon excitation at 399 nm (for NMM fluorescence) was measured in the presence of increasing concentrations of rpoB-WT (Figure 5). The signal intensity increases with the target concentration in the range of 0-1024 nM.

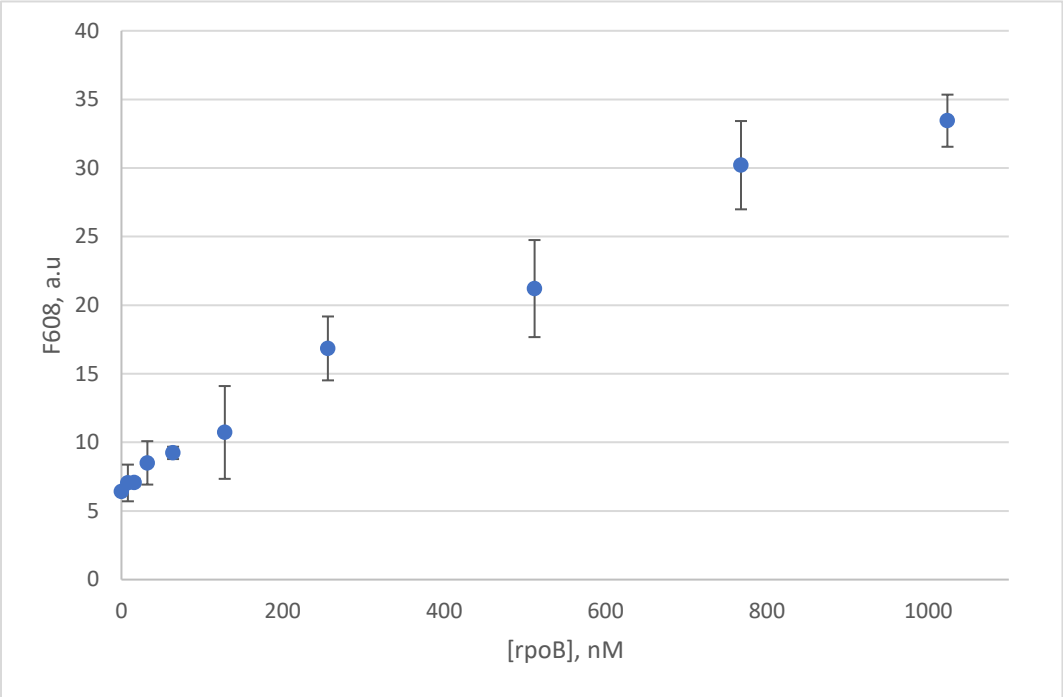

Figure 5. Fluorescence of NMM in the presence of the rpoB-specific SGQ probe as a function of rpoB_WT concentration (0-1024 nM). The data shown was an average from three independent experiments, and error bars are provided as standard deviations from the average.

Linear dynamic range for the rpoB detection with the cognate rpoB_WT is 1-768 nM. The LOD and LOQ were determined from the data in the presence of 0-64 nM rpoB_WT (Figure 6) using the 3σ/S and 10σ/S rule, respectively (Dolatto, 2012). For the probe, the LOD of 160 ± 15 nM and the LOQ of 540 ± 52 nM was calculated.

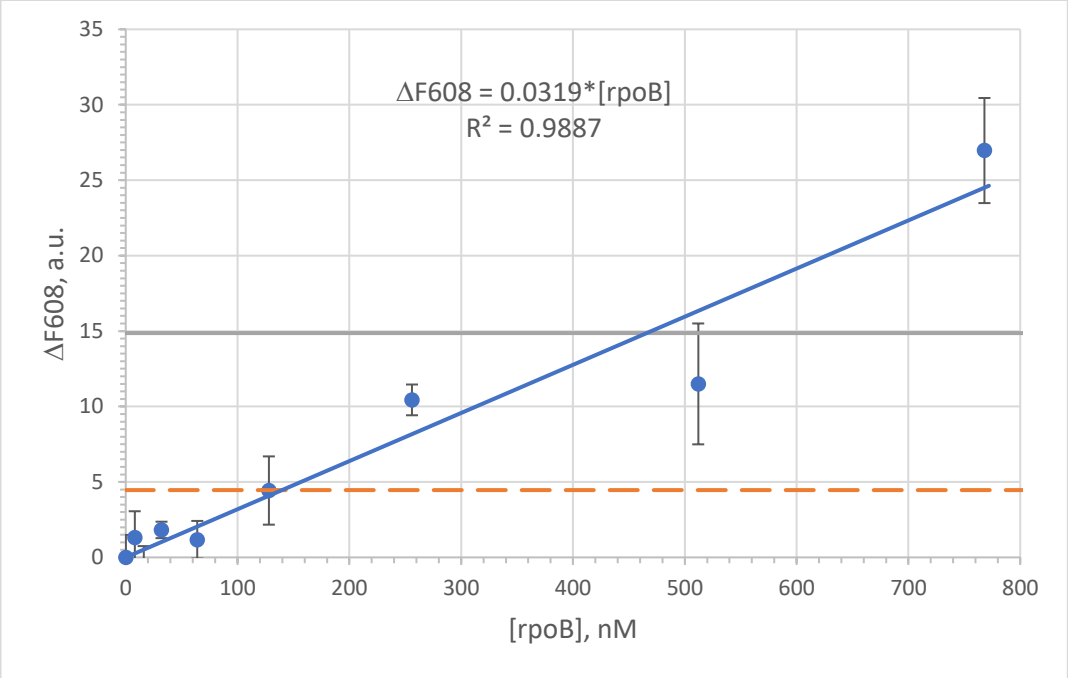

Figure 6. Linear dynamic range for the rpoB-specific SGQ probe. The fluorescence thresholds corresponding to LOD and LOQ are shown with orange dotted and grey dashed lines, respectively. The data of four independent experiments is averaged. The error bars are given as standard deviations from the average. The signal is expressed in DF=F-F_{Blank}, where F_{Blank} is the signal in the absence of the target.

Next, the selectivity of the rpoB-specific SGQ probe was tested. Figure 7 shows the signal triggered by mismatched targets rpoB_C>G and rpoB_C>T as compared with the signal triggered by the cognate rpoB_WT target (Table 1). Even though the signal triggered by the mismatched targets was statistically lower than that in response to the wild-type sequence, still the response to non-specific target was higher than the background (Figure 7). The signal of the SGQ probe triggered by rpoB_C>T was much higher than that for rpoB_C>G. This is explained by the formation of a G-T wobble base pair in the probe-rpoB_C>T complex, which increases stability of the mismatched complex.

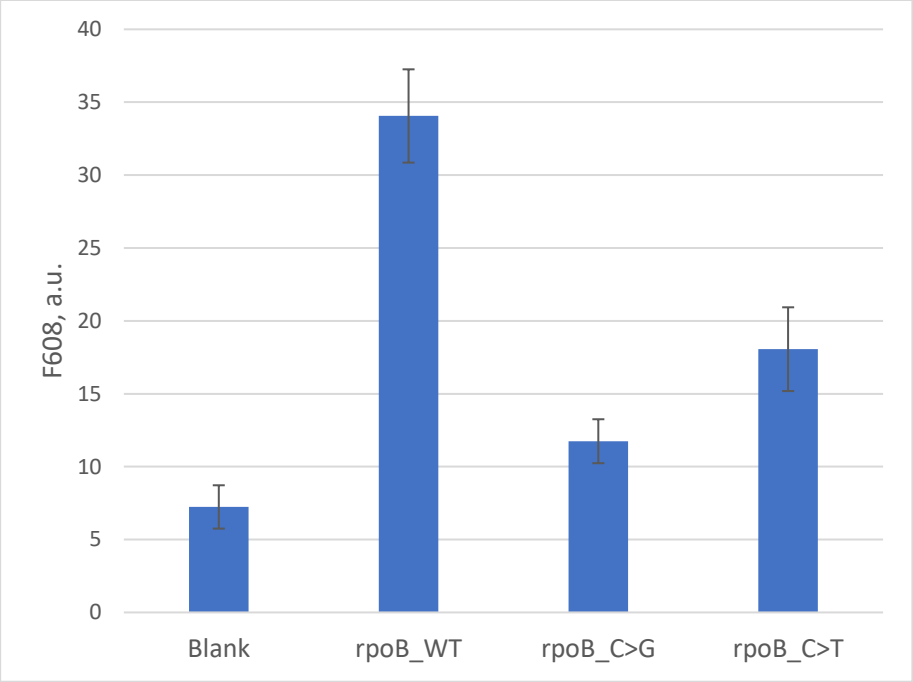

Figure 7. Selectivity of the rpoB-specific probe using NMM as a signal indicator. The targets (either specific rpoB_WT, single nucleotide substituted rpoB_C>G and single nucleotide substituted rpoB_C>T) were at 1 μM. Blank represents the sample of the probe in the absence of the targets. The data of at least three independent experiments was averaged, and the standard deviations were shown as error bars.

3.4 Multiplex Assay

Having demonstrated good selectivity of the split aptamer probes in detecting their cognate targets, we explored the probes' application in a multiplex format. The SDA and SGQ probes and their specific dye indicators (AO and NMM, respectively) were mixed together in the absence of the targets or in the presence of different combinations of katG_WT and rpoB_WT. In addition, each probe was assayed with the same target combinations individually. Fluorescence of all samples was measured under two conditions: (1) upon excitation at 399 nm to elicit NMM fluorescence with a maximum around 608 nm, and (2) upon excitation at 475 nm to elicit AO fluorescence with a maximum around 540 nm. For conditions (1), high signal was expected for the samples containing the SGQ probe if rpoB_WT was present. Under conditions (2), high AO fluorescence was expected only for the samples containing both the SDA probe and katG_WT. As can be seen

from Figure 8, the results obtained in the experiment match the expected pattern. At the same time, for NMM fluorescence, relatively high signal was observed for presumably low-fluorescent samples containing the katG_WT-specific SDA probe only, or both SDA and SGD probes, in the presence of katG_WT only (Figure 8A, grey bars for the first and last bar groups). This increase in fluorescence can be explained by promiscuous binding of DA to several fluorogenic dyes including NMM, which has been previously noticed in our laboratory (Connelly et al., 2021). As for the AO signal, decreased fluorescence of the sample containing both targets with only one probe (SDA), as compared to that for the sample with both probes present, was observed (Figure 8B, blue bars for the first and last bar groups). This limitation is irrelevant for multiplex application though. In the multiplex format, the presence of the cognate target, either alone or in mixture with the non-cognate target, the AO fluorescence enhanced more than 25-fold from the no-target sample or sample with only the non-cognate target (Figure 8B).

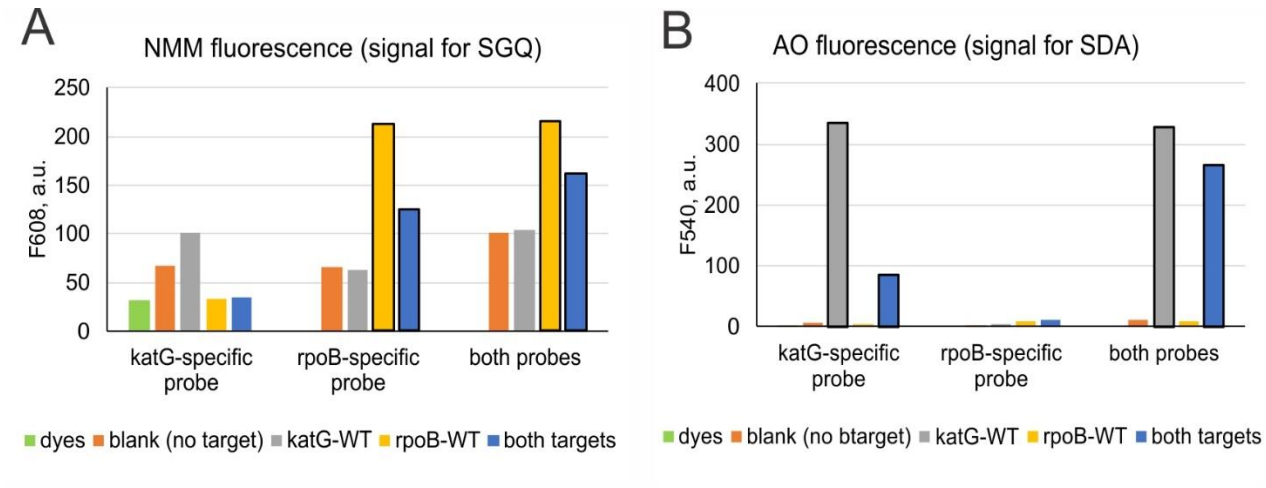

Figure 8. Response of the katG_WT-specific SDA probe and rpoB_WT-specific SGQ probe to different target combinations when the probes were used either separately or in a multiplex format. Signal was measured at 608 nm upon excitation at 399 nm for NMM fluorescence (positive signal for the SGQ probe) (A) or at 540 nm upon excitation at 475 nm for AO fluorescence (positive signal for the SDA probe) (B). The signal expected to be high is designated by the bars bordered in black.

We also recorded full emission spectra in the range of 420-640 nm and 520-640 nm when excited at 399 nm and 475 nm, respectively, for the samples containing both SDA and SGQ probes. As seen in Figure 9, even upon excitation at 399 nm, emission maximum at 540 nm is observed for the samples expected to have high AO fluorescence. This is due to the existence of an absorption band around 390 nm characteristic for AO in the presence of DA (Figure 10). The intensity of the 540-nm emission band upon 399-nm excitation is lower than under the excitation conditions (at 475 nm) optimized for AO (Figure 9, Inset). Nevertheless, this band is only present in the spectra of the samples, which also exhibited high signal at 540 nm upon excitation at 475 nm ideal for the AO-DA system (Figure 9).

Observance of emission of both AO and NMM dyes at the same excitation wavelength opens a perspective to visually monitor the signal if a proper UV light source is used. Figure 11 shows tube images for the samples containing both probes in the presence of different target combinations. A pink hue with the presence of rpoB_WT and a green hue with katG_WT present can be seen with the naked eye. When both targets are present, the green turns slightly more pink, which can be explained by the higher intensity of AO fluorescence triggered by katG_WT muting the pink hue.

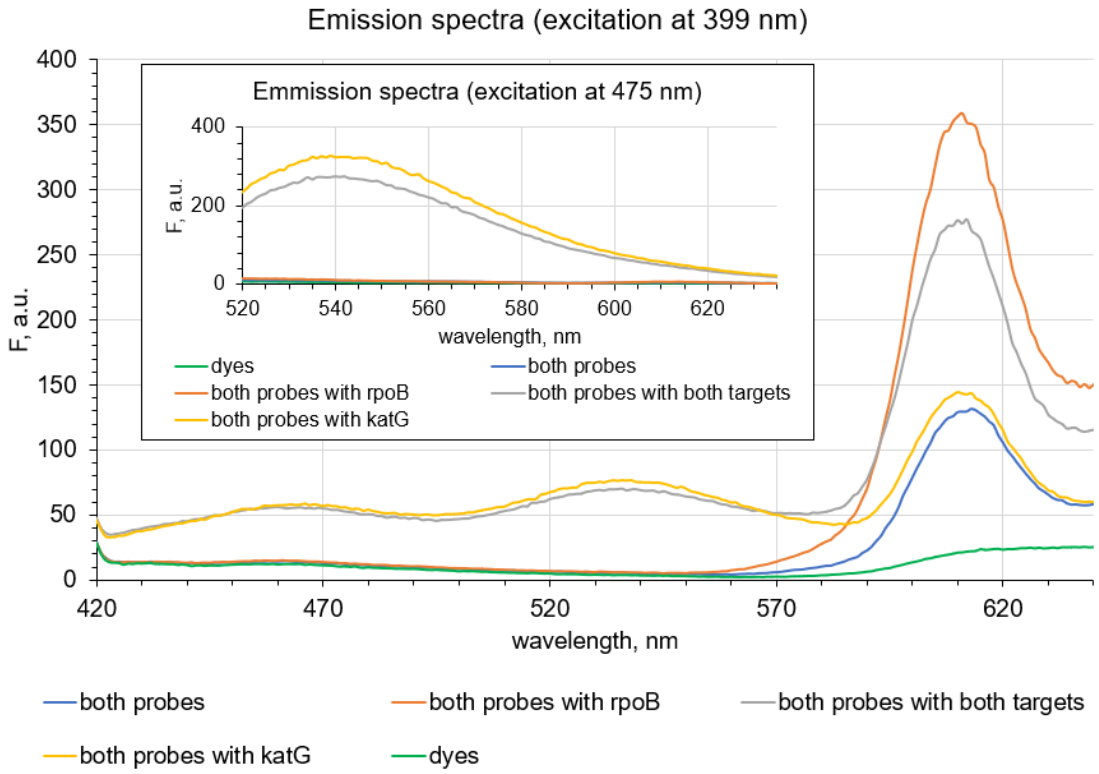

Figure 9. Fluorescence emission spectra for the samples containing AO, NMM, and/or both SDA and SGQ probes in the absence or presence of different combinations of katG-WT and rpoB_WT (excitation at 399 nm). *Inset.* The same samples excited at 475 nm.

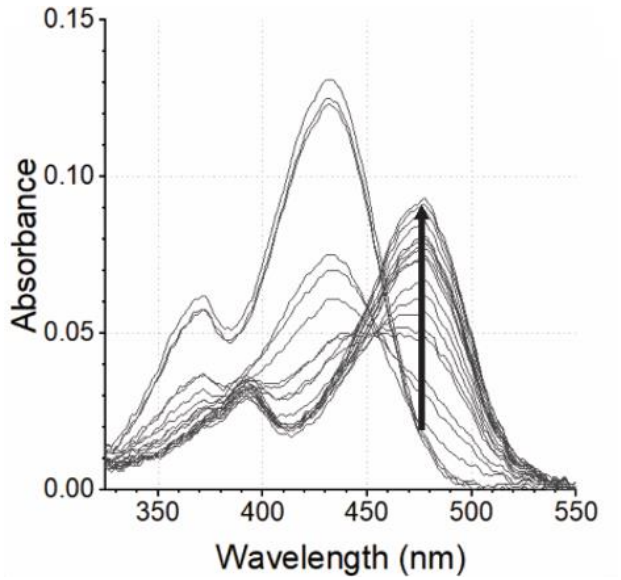

Figure 10. Absorbance spectra for AO (7.5 µM) in the presence of increasing concentrations (0-7.5 µM) of DA (Connelly et al., 2021). Changes in the spectra upon addition of the aptamer are indicated by the arrow.

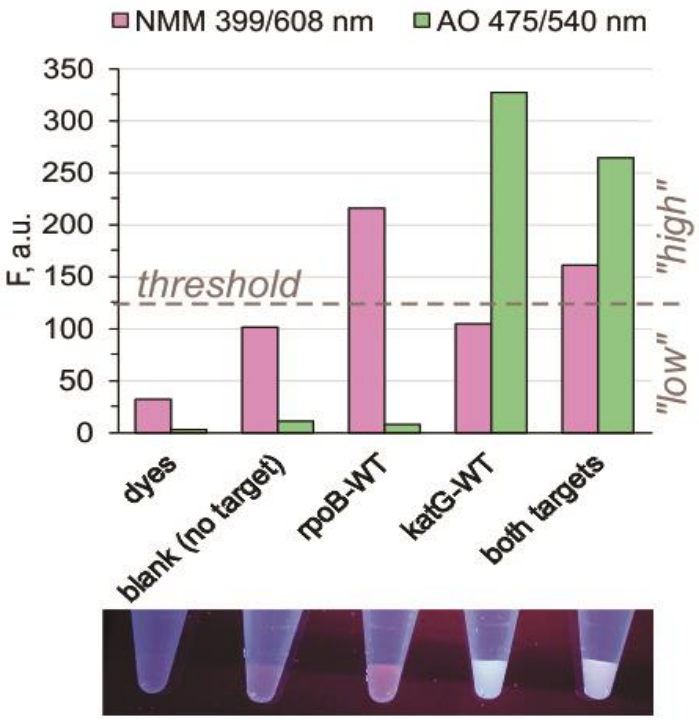

Figure 11. Response of the SDA and SGQ probes mixed together in the presence of both AO and NMM dyes to rpoB_WT, katG_WT or both targets simultaneously. As controls, samples containing dyes only or the dyes with the probes in the absence of targets were measured. The samples were excited at 399 nm to detect emission at 608 nm, or at 475 nm to detect emission at 540 nm. Images of the tubes containing the samples are shown below the bar graph. The images were taken using a smartphone camera upon excitation at 365 nm using a UV transilluminator.

CHAPTER 4: DISCUSSION

Drug-susceptibility testing (DST) has become an integral part of diagnosing bacterial infections. For slow-growing pathogens like *M. tuberculosis,* culture-based phenotypic DST fails to provide timely information regarding the pathogen's drug susceptibility profile (Kim 2005), thereby urging for genotypic DST tools. Since one of the mechanisms used by bacteria to develop drug resistance is through acquisition of point-mutations in bacterial genes, sequence-specific probes utilized for genotypic DST need to exhibit excellent selectivity and discriminate between point mutations. Examples of currently available techniques for detection of drug-resistant *Mycobacterium tuberculosis*, for example, include GenoType MTBDR*plus* line probe assay (Meaza et al., 2017), which allows for identification of mycobacterial strains resistant to rifampin and/or isoniazid, but involves multiple manipulations and specialized equipment. Another example is the Xpert MTB/RIF Ultra assay (Chakravorty et al. 2017), which is a cartridge-based system with minimal manual steps. At the same time, the Xpert assay only analyzes the pathogens in terms of rifampin resistance and relies on multiple probes, each of which is doubly conjugated with dyes.

In attempt to decrease the cost of the test for MDR-TB detection, some research groups combined isothermal amplification methods with user-friendly signal reporting systems. For example, Pavankumar and colleagues employed rolling circle amplification (RCA) in conjunction with padlock probes and signal detection by a lateral flow assay for isothermal amplification and analysis of point mutations in codon 315 of the katG gene and codon 531 of the rpoB gene of *M. tuberculosis* (Pavankumar et al. 2016). Despite an attractive implementation and time to results comparable to that of the Xpert MTB/RIF Ultra assay (75 min), the test required as high as 30 ng of mycobacterial DNA for reliable genotyping results. Another disadvantage is the need to use

gold nanoparticles conjugated oligonucleotide probes for signal visualization of the lateral flow strips.

In this project, we have characterized label-free split aptamer probes capable of discriminating nucleic acid targets down to single-nucleotide differences. The probes take advantage of fluorescent light-up DNA aptamers – dapoxyl binding aptamer, which can also turn on fluorescence of AO dye, and NMM-binding G-quadruplex based DNA aptamer – as signal transducers. The SDA probe exhibits the single digit nanomolar LOD and LOQ (Figure 2), which is similar to those of the MB probes (Kolpashchikov 2012). The LOD and LOQ for the SGQ probe is ~20-times higher than those for the SDA probe (Figure 6). For both probes to be usable for pathogen detection, amplification of bacterial nucleic acids is required. Previously, the SDA probe was successfully paired with nucleic acid sequence-based amplification (NASBA) (Kikuchi et al. 2019, Connelly et al. 2021). We anticipate that the SGQ/NMM system is also compatible with the NASBA reaction based on the data obtained in our laboratory for instantaneous nucleic acid analysis using a transcription-based system expressing GQ sequence (unpublished data).

Remarkably, the two probes can work together with minimal interference, and the expected signal pattern is observed in the presence of the targets specific to each probe both individually and in mixture. The signal can be observed both with the help of a fluorometer (Figure 9) and visually, with an unaided eye (Figure 11, tube images). Both fluorophores (AO and NMM), when bound to the probe in the presence of the cognate target, can be excited under the same conditions (Figures 9 and 11), thus enabling an easy single readout protocol. The latter is an attractive property of a molecular assay. For example, to create wavelength-shifting molecular beacon probes that fluoresce at different emission wavelength while excited by a common

monochromatic light source, covalent modification of already double-labeled oligonucleotide probe with a third fluorophore was required (Tyagi et al. 2000). In our multiplex assay, the same scenario was realized without the need of conjugating the probe with dyes.

CHAPTER 5: CONCLUSION

We have demonstrated that split aptamer probes based on dapoxyl aptamer or an NMM-binding G-quadruplex sequence – SDA and SGQ probes, respectively, - can selectively differentiate between nucleic acid targets with point-mutations, which can be applicable to molecular drug-susceptibility testing of bacterial pathogens, as proved in this work using target sequences from *M. tuberculosis.* When used separately, SDA and SGQ probes exhibit the LOD/LOQ for their cognate targets to be (2.6 ± 0.6 nM)/(9 ± 2 nM) and (160 ± 15 nM)/(540 ± 52 nM), respectively. The mutant targets triggered the signal at or below the background level for the SDA probe, thus proving excellent selectivity of the split probe approach. When used in a multiplex format, the probes demonstrated high signal only in response to the presence of their cognate target. The signal could be detected visually and differentiated by the color upon excitation of fluorescence using a UV transilluminator or a handheld UV light source. These probes can be implemented in diagnostics of infectious diseases at a point-of-care if combined with isothermal amplification of pathogens' DNA/RNA from clinical samples.

REFERENCES

Alam, K. K.; Tawiah, K. D.; Lichte, M. F.; Porciani, D.; Burke, D. H. A Fluorescent Split Aptamer for Visualizing RNA–RNA AssemblyIn Vivo. *ACS Synthetic Biology* **2017**, *6* (9), 1710–1721.

Almeida Da Silva, P. E.; Palomino, J. C. Molecular Basis and Mechanisms of Drug Resistance in Mycobacterium Tuberculosis: Classical and New Drugs. *Journal of Antimicrobial Chemotherapy* **2011**, *66* (7), 1417–1430.

Bonnet, G.; Tyagi, S.; Libchaber, A.; Kramer, F. R. Thermodynamic Basis of the Enhanced Specificity of Structured DNA Probes. *Proceedings of the National Academy of Sciences* **1999**, *96* (11), 6171–6176.

Chakravorty, S.; Simmons, A. M.; Rowneki, M.; Parmar, H.; Cao, Y.; Ryan, J.; Banada, P. P.; Deshpande, S.; Shenai, S.; Gall, A.; Glass, J.; Krieswirth, B.; Schumacher, S. G.; Nabeta, P.; Tukvadze, N.; Rodrigues, C.; Skrahina, A.; Tagliani, E.; Cirillo, D. M.; Davidow, A.; Denkinger, C. M.; Persing, D.; Kwiatkowski, R.; Jones, M.; Alland, D. The New Xpert MTB/RIF Ultra: Improving Detection of Mycobacterium Tuberculosis and Resistance to Rifampin in an Assay Suitable for Point-of-Care Testing. *mBio* **2017**, *8* (4).

Connelly, R. P.; Madalozzo, P. F.; Mordeson, J. E.; Pratt, A. D.; Gerasimova, Y. V. Promiscuous Dye Binding by a Light-up Aptamer: Application for Label-Free Multi-Wavelength Biosensing. *Chemical Communications* **2021**, *57* (30), 3672–3675.

Connelly, R. P.; Morozkin, E. S.; Gerasimova, Y. V. Cover Feature: Alphanumerical Visual Display Made of DNA Logic Gates for Drug Susceptibility Testing of Pathogens (ChemBioChem 3/2018). *ChemBioChem* **2018**, *19* (3), 198–198.

Davies, J. E. Origins, Acquisition and Dissemination of Antibiotic Resistance Determinants. *Ciba Foundation Symposium 207 - Antibiotic Resistance: Origins, Evolution, Selection and Spread* **2007**, 15–35.

Demidov, V. V.; Frank-Kamenetskii, M. D. Two Sides of the Coin: Affinity and Specificity of Nucleic Acid Interactions. *Trends in Biochemical Sciences* **2004**, *29* (2), 62–71.

Dolatto, R. G.; Messerschmidt, I.; Pereira, B. F.; Silveira, C. A.; Abate, G. Determination of Phenol and o-Cresol in Soil Extracts by Flow Injection Analysis with Spectrophotometric Detection. *Journal of the Brazilian Chemical Society* **2012**, *23* (5), 970–976.

Gerasimova, Y. V.; Kolpashchikov, D. M. Folding of 16S RRNA in a Signal-Producing Structure for the Detection of Bacteria. *Angewandte Chemie International Edition* **2013**, *52* (40), 10586–10588.

Helb, D.; Jones, M.; Story, E.; Boehme, C.; Wallace, E.; Ho, K.; Kop, J. A.; Owens, M. R.; Rodgers, R.; Banada, P.; Safi, H.; Blakemore, R.; Lan, N. T.; Jones-López, E. C.; Levi, M.; Burday, M.; Ayakaka, I.; Mugerwa, R. D.; McMillan, B.; Winn-Deen, E.; Christel, L.; Dailey, P.; Perkins, M. D.; Persing, D. H.; Alland, D. Rapid Detection OfMycobacterium Tuberculosisand Rifampin Resistance by Use of On-Demand, Near-Patient Technology. *Journal of Clinical Microbiology* **2009**, *48* (1), 229–237.

Kato, T.; Shimada, I.; Kimura, R.; Hyuga, M. Light-up Fluorophore–DNA Aptamer Pair for Label-Free Turn-on Aptamer Sensors. *Chemical Communications* **2016**, *52* (21), 4041–4044.

Kikuchi, N.; Kolpashchikov, D. M. Split Spinach Aptamer for Highly Selective Recognition of DNA and RNA at Ambient Temperatures. *ChemBioChem* **2016**, *17* (17), 1589–1592.

Kikuchi, N.; Reed, A.; Gerasimova, Y. V.; Kolpashchikov, D. M. Split Dapoxyl Aptamer for Sequence-Selective Analysis of Nucleic Acid Sequence Based Amplification Amplicons. *Analytical Chemistry* **2019**, *91* (4), 2667–2671.

Kim, S. J. Drug-Susceptibility Testing in Tuberculosis: Methods and Reliability of Results. *European Respiratory Journal* **2005**, *25* (3), 564–569.

Klug, S. J.; Famulok, M. All You Wanted to Know about SELEX. *Molecular Biology Reports* **1994**, *20* (2), 97–107.

Kolpashchikov, D. M. An Elegant Biosensor Molecular Beacon Probe: Challenges and Recent Solutions. *Scientifica* **2012**, *2012*, 1–17.

Kolpashchikov, D. M. Binary Probes for Nucleic Acid Analysis. *Chemical Reviews* **2010**, *110* (8), 4709–4723.

Larios-Sanz, M., Kourentzi, K. D., Warmflash, D., Jones, J., Pierson, D. L., Willson, R. C., & Fox, G. E. 16S rRNA beacons for bacterial monitoring during human space missions. *Aviation, space, and environmental medicine* **2007**, *78*(4), A43-A47.

Köhler, O.; Jarikote, D. V.; Seitz, O. Forced Intercalation Probes (FIT Probes): Thiazole Orange as a Fluorescent Base in Peptide Nucleic Acids for Homogeneous Single-Nucleotide-Polymorphism Detection. *ChemBioChem* **2004**, *6* (1), 69–77.

Meaza, A.; Kebede, A.; Yaregal, Z.; Dagne, Z.; Moga, S.; Yenew, B.; Diriba, G.; Molalign, H.; Tadesse, M.; Adisse, D.; Getahun, M.; Desta, K. Evaluation of Genotype MTBDRplus VER 2.0 Line Probe Assay for the Detection of MDR-TB in Smear Positive and Negative Sputum Samples. *BMC Infectious Diseases* **2017**, *17* (1).

N-Methyl mesoporphyrin IX. https://pubchem.ncbi.nlm.nih.gov/compound/656404 (accessed Apr 25, 2021).

NAVANI, N.; LI, Y. Nucleic Acid Aptamers and Enzymes as Sensors. *Current Opinion in Chemical Biology* **2006**, *10* (3), 272–281.

Neubacher, S.; Hennig, S. RNA Structure and Cellular Applications of Fluorescent Light-Up Aptamers. *Angewandte Chemie International Edition* **2018**, *58* (5), 1266–1279.

Nikaido, H. Multidrug Resistance in Bacteria. *Annual Review of Biochemistry* **2009**, *78* (1), 119–146.

Pavankumar, A. R.; Engström, A.; Liu, J.; Herthnek, D.; Nilsson, M. Proficient Detection of Multi-Drug-Resistant Mycobacterium Tuberculosis by Padlock Probes and Lateral Flow Nucleic Acid Biosensors. *Analytical Chemistry* **2016**, *88* (8), 4277–4284.

Rossetti, M.; Del Grosso, E.; Ranallo, S.; Mariottini, D.; Idili, A.; Bertucci, A.; Porchetta, A. Programmable RNA-Based Systems for Sensing and Diagnostic Applications. *Analytical and Bioanalytical Chemistry* **2019**, *411* (19), 4293–4302.

Stancescu, M.; Fedotova, T. A.; Hooyberghs, J.; Balaeff, A.; Kolpashchikov, D. M. Nonequilibrium Hybridization Enables Discrimination of a Point Mutation within 5–40 °C. *Journal of the American Chemical Society* **2016**, *138* (41), 13465–13468.

Sypabekova, M.; Bekmurzayeva, A.; Wang, R.; Li, Y.; Nogues, C.; Kanayeva, D. Selection, Characterization, and Application of DNA Aptamers for Detection of Mycobacterium Tuberculosis Secreted Protein MPT64. *Tuberculosis* **2017**, *104*, 70–78.

Tuberculosis (TB). https://www.who.int/news-room/fact-sheets/detail/tuberculosis (accessed Apr 25, 2021).

Tyagi, S.; Kramer, F. R. Molecular Beacons: Probes That Fluoresce upon Hybridization. *Nature Biotechnology* **1996**, *14* (3), 303–308.

Verduzco, C.; Farnell, S.; Yishay, T.; Gerasimova, Y. V. Toward a Rational Approach to Design Split G-Quadruplex Probes. *ACS Chemical Biology* **2019**, *14* (12), 2701–2712.

Versalovic, J.; Lupski, J. R. Molecular Detection and Genotyping of Pathogens: More Accurate and Rapid Answers. *Trends in Microbiology* **2002**, *10* (10).

Wang, D. G. Large-Scale Identification, Mapping, and Genotyping of Single-Nucleotide Polymorphisms in the Human Genome. *Science* **1998**, *280* (5366), 1077–1082.

Yett, A.; Lin, L. Y.; Beseiso, D.; Miao, J.; Yatsunyk, L. A. N-Methyl Mesoporphyrin IX as a Highly Selective Light-up Probe for G-Quadruplex DNA. *Journal of Porphyrins and Phthalocyanines* **2019**, *23* (11n12), 1195–1215.

Zadeh, J. N.; Steenberg, C. D.; Bois, J. S.; Wolfe, B. R.; Pierce, M. B.; Khan, A. R.; Dirks, R. M.; Pierce, N. A. NUPACK: Analysis and Design of Nucleic Acid Systems. *Journal of Computational Chemistry* **2010**, *32* (1), 170–173.